International Journal of Heat and Mass Transfer 52 (2009) 5090–5101

Contents lists available at ScienceDirect

International Journal of Heat and Mass Transfer

journal homepage: www.elsevier.com/locate/ijhmt

An experimental study on the effect of ultrasonication on viscosity and heat transfer performance of multi-wall carbon nanotube-based aqueous nanofluids

Paritosh Garg [a], Jorge L. Alvarado [b,*], Charles Marsh [c,d], Thomas A. Carlson [c], David A. Kessler [e], Kalyan Annamalai [a]

[a] Department of Mechanical Engineering, Texas A&M University, College Station, TX 77843, USA
[b] Department of Engineering Technology and Industrial Distribution, Texas A&M University, 117 Thompson Hall, 3367 TAMU, College Station, TX 77843-3367, USA
[c] U.S. Army, Engineer Research and Development Center, Construction Engineering Research Laboratory, 2902 Newmark, Drive, Champaign, IL 61822-1076, USA
[d] Department of Nuclear, Plasma, and Radiological Engineering, 216 Talbot Laboratory, MC-234, 104 South Wright Street, Urbana, IL 61801, USA
[e] Laboratory for Computational Physics and Fluid Dynamics, Naval Research Laboratory, Code 6404, 4555 Overlook Ave. SW, Washington, DC 20375, USA

ARTICLE INFO

Article history:
Received 21 May 2008
Received in revised form 17 April 2009
Accepted 17 April 2009
Available online 17 June 2009

Keywords:
Convective heat transfer
Nanofluids
Multi-walled
Carbon nanotubes
Thermal conductivity
Viscosity
Heat transfer enhancement
Non-Newtonian fluid
TEM

ABSTRACT

Four samples of 1 wt% multi-walled carbon nanotube-based (MWCNT) aqueous nanofluids prepared via ultrasonication were thermally characterized. Direct imaging was done using a newly developed wet-TEM technique to assess the dispersion state of carbon nanotubes (CNT) in suspension. The effect of dispersing energy (ultrasonication) on viscosity, thermal conductivity, and the laminar convective heat transfer was studied. Results indicate that thermal conductivity and heat transfer enhancement increased until an optimum ultrasonication time was reached, and decreased on further ultrasonication. The suspensions exhibited a shear thinning behavior, which followed the Power Law viscosity model. The maximum enhancements in thermal conductivity and convective heat transfer were found to be 20% and 32%, respectively. The thermal conductivity enhancement increased considerably at temperatures greater than 24 °C. The enhancement in convective heat transfer was found to increase with axial distance. A number of mechanisms related to boundary layer thickness, micro-convective effect, particle rearrangement, possible induced convective effects due to temperature and viscosity variations in the radial direction, and the non-Newtonian nature of the samples are discussed.

1. Introduction

Managing high thermal loads has become very critical in the rapid developed infrastructure, industrial, transportation, defense, space sectors. Several cooling technologies have been researched recently. Conventional heat transfer techniques that rely on fluids like water, ethylene glycol, and mineral oils continue to be popular due to its simple nature. Conventional heat transfer systems used in applications like petrochemical, refining, and power generation are rather large and involve significant amount of heat transfer fluids. In certain cooling applications, small heat transfer systems are required. These applications have a critical relationship between size of a mechanical system and the cost associated with manufacturing and operation. Improvements could be made in the existing heat transfer systems by enhancing the performance of heat transfer fluids resulting in lesser heat exchanger surface area, lower capital costs, and higher energy efficiencies. In this pursuit, numerous techniques to enhance the thermal performance of heat transfer fluids have been investigated. One of the methods used is to add nanoparticles of highly thermally conductive materials like carbon, metal, metal oxides into heat transfer fluids to improve the overall thermal conductivity. Nanoparticles could be either spherical or cylindrical. Carbon nanoparticles of cylindrical form are called carbon nanotubes (CNT). One type of carbon nanotube is called multi-walled carbon nanotubes (MWCNT) because they have multiple concentric tubes in a single configuration.

This study is concerned with nanofluids prepared by dispersing MWCNT in water, and their potential use as heat transfer fluids in a host of applications. It has now been established that when carbon nanotubes are suspended in conventional heat transfer fluids, enhancements in thermal conductivity and convective heat transfer performance are observed [1–5]. The motivations behind the current study are as follows. Firstly, there is limited information about the effect of preparation and processing conditions on the physical properties and thermal performance of CNT aqueous nanofluids. Secondly, limited experimental data is currently available for CNT-based nanofluids particularly in the area of viscosity. Lastly, only two studies have been reported to date on convective heat transfer of aqueous CNT nanofluids [4,6]. Convective heat

* Corresponding author. Tel.: +1 979 458 1900; fax: +1 979 862 7969.
E-mail address: alvarado@entc.tamu.edu (J.L. Alvarado).

0017-9310/$ - see front matter © 2009 Elsevier Ltd. All rights reserved.
doi:10.1016/j.ijheatmasstransfer.2009.04.029

Nomenclature

K	flow consistency index, mPa s
n	flow behavior index
N	rotational speed, rpm
k	fluid thermal conductivity, W/m °C
x	axial distance from the inlet of the test section, m
h	convective heat transfer coefficient, W/m^2 °C
q''_s	heat flux applied to the fluid, W/m^2
T_s	surface temperature, °C
T_b	fluid bulk temperature, °C
P	inner perimeter of the copper tube, m
$\dot{m}$	mass flow rate, kg/s
c_p	fluid specific heat, kJ/kg °C
A	inner surface area of the copper tube, m^2
D_i	inside diameter of copper tube, m
Nu	Nusselt number
e	specific energy, J/g
d_p	particle diameter, m or μm
u	fluid velocity, m/s
L	heated length, cm
a	particle radius, cm
Pr	Prandtl number
Re	Reynolds number, $\frac{\rho \cdot uD_i}{\mu}$
Pe	Peclet number, $\frac{\dot{\gamma}_f \cdot d_p^2}{\alpha_f}$

Greek symbols

τ	shear stress, N/m^2
$\dot{\gamma}$	shear rate, s^{-1}
τ'	yield shear stress, N/m^2
μ	fluid viscosity, mPa s
δ	hydrodynamic boundary layer thickness, m
δ_t	thermal boundary layer thickness, m
$\bar{\dot{\gamma}}_f$	local mean shear rate experienced by fluid, s^{-1}
α_f	fluid thermal diffusivity, m^2/s
ρ	fluid density, kg/m^3
ϕ	particle volume fraction
ω	angular velocity of particle, rad/s
v_f	kinematic viscosity, cm^2/s

Subscripts

p	particle
s	surface
b	bulk
i	inlet
o	outlet
f	fluid

transfer is an area which still needs to be completely explored and understood. In this study, an effort has been made to consider all the above factors in a way that would move forward nanofluid research to the next phase.

2. Background

2.1. Past research in CNT nanofluids preparation

One of the critical steps in preparing carbon nanofluids is dispersing carbon nanotubes in the base fluid. Due to the high aspect ratio of carbon nanotubes and strong Van der Waal's forces between carbon surfaces, dispersion of CNT in aqueous medium can be challenging. CNTs are hydrophobic in nature and thus cannot be dispersed in water under normal conditions. There are usually two methods to disperse carbon nanotubes in base fluids: mechanical and chemical [7]. Mechanical methods generally include ultrasonication using a probe or a bath. Chemical methods include using surfactants and CNT-functionalization using acids. The surfactant method changes the wetting or adhesion behavior which helps in reducing their tendency to agglomerate. Chemical functionalization generally involves treating CNTs with acids at high temperature. This results in addition of polar groups like –COOH or –OH at defect sites on nanotube surface, thus making CNTs more hydrophilic in nature. However, aggressive chemical functionalization, can damage the nanotubes. Both mechanical and chemical methods can reduce the aspect ratio distribution of the nanotubes. It has been reported that thermal conductivity enhancement in CNT nanofluids decreases with reduction in aspect ratio [1,8]; therefore, proper care still has to be taken during processing to minimize adverse effects. In this study, a combination of a mechanical method through ultrasonication, and a chemical method with surfactants were used.

Surfactants are used to disperse carbon nanotubes in several cases. Some examples of previously used surfactants are sodium dodecyl sulfate (SDS) [1], sodium dodecyl benzene sulfonate (SDBS) [2], hexadecyltrimethyl ammonium bromide (CTAB) [3] and Nanosperse AQ [3]. Through past studies, it was found that SDBS failed at elevated temperatures [2]. Additionally, Gum Arabic (GA) was found to be a better surfactant than sodium dodecyl sulfate (SDS) and cetyltrimethylammoniumchloride (CTAC) for dispersing carbon nanotubes in DI water [9]. This has been confirmed through testing where two samples of 1 wt% MWCNT aqueous suspensions were prepared using GA and SDS as surfactants. Suspensions prepared using GA were found to be visually more stable even after several weeks as compared to the ones prepared using SDS. Therefore, based on past and current research activities, GA was found to be the most suitable surfactant. However, GA has a tendency to increase viscosity when added to DI water. A highly viscous nanofluid could also result in increased pumping power for commercial applications. Therefore, it is important that the amount added is optimum.

2.2. Past research on viscosity of CNT nanofluids

Viscosity of a heat transfer fluid is important with respect to studying its convective heat transfer and pumping power required for practical applications. Optimization is required between heat transfer capability and the viscosity as it has a direct bearing on the design of flow and heat transfer equipment. Experimental data for the effective viscosity of aqueous nanofluids is limited to certain nanoparticles, such as Al_2O_3 [10–13], CuO [13,14], TiO_2 [10] and MWCNT [4]. Most of these studies have been directed towards metal oxide nanoparticles and there is only one work which studied aqueous MWCNT extensively [4]. The parameters against which viscosity has been studied until today include particle volume concentration, temperature and shear rate. Empirical and accurate analytical models for prediction of the viscosity of high aspect ratio nanofluids are not currently available. Those studies are mainly focused on spherical nanoparticles of metal oxides, and have their basis from the Einstein theory for viscosity [15] which takes into account spherical particles. In the case of CNT nanofluids, such models cannot correlate the experimental data well because the shape of CNTs does not satisfy the assumptions in the Einstein model.

Aqueous CNT nanofluids have shown to exhibit shear thinning or pseudoplastic type of non-Newtonian behavior [4]. However, no study has been reported that correlates empirical data of CNT nanofluids with theoretical non-Newtonian viscosity models. The theoretical models provide equations that correlate shear stress of a flowing fluid to shear rate. This helps in classifying the flow behavior of a new nanofluid. The widely used models for non-Newtonian flow are Power Law, $\tau = K \cdot \dot{\gamma}^n$ and Herschel Bulkley, $\tau = \tau' + K \cdot \dot{\gamma}^n$ where $\tau, K, \dot{\gamma}, \tau'$ and n are shear stress, flow consistency index, shear rate, yield shear stress and flow behavior index, respectively.

Additionally, no work has been done in studying the effect of processing or ultrasonication time on the viscosity of MWCNT aqueous nanofluids. Experimental work in this area could provide impetus to theoretical model development for CNT nanofluids. In this work, an effort has been made to study this effect by fitting the experimental data in the form of a shear stress-shear rate mathematical model.

2.3. Past research on thermal conductivity of CNT nanofluids

The heat transfer characteristic of a flowing fluid can be represented by a Nusselt number, which takes into account the Prandtl number including thermal conductivity. Thus, a first assessment of the heat transfer potential of a nanofluid is to measure its thermal conductivity. To date, a lot of research data has been published in this area for metal oxide nanofluids but comparatively less for CNT nanofluids [11,16,17]. One of the first studies involving CNT nanofluids was by Choi et al. [5]. They measured the effective thermal conductivity of MWCNTs dispersed in synthetic poly(α-olefin) oil and reported a thermal conductivity enhancement of 160% by 1.0 vol % nanotubes in oil. Subsequently, data was published by Xie et al. [18] where enhancements were reported for water, ethylene glycol and decene as base fluids. Assael et al. [1,3] data focused on aqueous MWCNT nanofluids with SDS, CTAB and Nanosperse AQ as dispersants. However, both studies reported much less enhancements as compared to those reported by Choi et al. [5]. The maximum thermal conductivity enhancement observed by Xie et al. [18] was only 20% for 1% nanotubes in decene by volume, and that observed by Assael et al. [1] was 38% for 0.6% CNTs in water by volume. In 2004, Wen and Ding [2] published data using SDBS as the dispersant. Their results were comparable to Xie et al. [18] and Assael et al. [1] and suggested that differences in interfacial resistances and thermal conductivities of carbon nanotubes used were the main reasons for the observed discrepancies with respect to Choi et al. [5]. Additionally, the base fluid used by Choi et al. [5] was poly-α-olefin (a lower thermal conductivity than water), though percentage enhancement reported was high, the absolute enhancement was not as high as expected. As SDBS was also found to fail at elevated temperatures, another set of data was published using GA as dispersant by Ding et al. [4]. In their study, a maximum enhancement of 79% was reported at 1 wt% MWCNT in water.

To date, most of the published data in MWCNT based nanofluids is focused on the thermal conductivity enhancement as a function of particle volume concentration, base fluid, and temperature. Effects of particle size [1,3], dispersant (surfactant) [1,3] and acidity [4] have also been considered. Assael et al. [3] reported the effect of particle size indirectly by increasing the homogenization time by ultrasonication, and concluded that when carbon nanotube suspensions are homogenized for long periods of time, their aspect ratio decreases, which subsequently decreases their thermal conductivity enhancements. Yang et al. [19] conducted similar studies and reached analogous conclusions with oil dispersions. However, no other studies have been found to confirm these findings. In the present study, thermal conductivity data with respect to ultrasonication time and temperature are presented.

Thermal conductivity enhancement in carbon nanotube dispersions is still not completely understood. Several mechanisms and phenomena have been postulated that attempt to explain the observed enhancements. Studies have indicated that nanotubes conduct current and heat ballistically or in fast diffusive manner [20]. The ballistic conduction is associated with the large phonon mean-free path in nanotubes. Hence, carbon nanotubes should promote faster heat diffusion in liquids. Furthermore, there is evidence that an organized solid-like structure of a liquid at the interface is a potential governing mechanism in heat conduction from a solid wall to an adjacent liquid [21]. It has been postulated [5] that this organized solid/liquid interface structure causes a favorable heat transport across the solid–liquid interface. Additionally, Jang and Choi [22] postulated another theory using Brownian motion of nanoparticles as a potential mechanism for increased thermal conductivity of nanofluids at elevated temperatures. It suggested that as temperature is increased, the viscosity of base fluids is decreased and Brownian motion of nanoparticles is consequently increased. It has been postulated that convection-like effects are induced by Brownian motion which result in increased apparent thermal conductivities. However, Keblinski et al. [23] showed that Brownian motion is unlikely to have direct role in the enhancement of thermal conductivity. Wen and Ding [2] suggested nanotube networking as one of the likely mechanisms that facilitates avenues for faster diffusion and potential ballistic transport of energy carriers. From all those studies, it is difficult to agree upon a single most important mechanism that solely contributes to enhanced thermal conductivity.

2.4. Past research on convective heat transfer of CNT nanofluids

The practical utility of nanofluids as heat transfer fluids is best determined by its convective heat transfer coefficient. Unlike past research activities which have focused on thermal conductivity, the study of convective heat transfer of nanofluids still needs to be explored in more detail. Only few papers have been written in this area, and most of them focused on metal oxide nanoparticles [10,11,16,17]. To date, only two papers have presented results from MWCNT aqueous suspensions under constant heat flux and laminar flow conditions. Faulkner et al. [6] reported heat transfer enhancement in a microchannel at very low Reynolds number (2–17) and particle volume concentrations between 1.1–4.4 vol %. Ding et al. [4] reported heat transfer enhancement at intermediate Reynolds number (800–1200) and low particle volume concentration (0.05 vol %). Although both of these papers reported heat transfer enhancement, however, the heat transfer enhancement trends with respect to particle volume concentration in one paper was found to contradict the other work. Therefore, it can be said that substantial amount of work is still required in this area. Both these papers considered parametric effects of particle volume concentration, Reynolds number and heat flux on the heat transfer enhancement. However, ultrasonication time or particle size reduction was not considered in those studies. As experimental research in this area is still new, theoretical models for heat transfer enhancement are quite limited too.

3. Experimental design

3.1. Sample preparation

De-ionized (DI) water, Gum Arabic (GA) and multi-walled carbon nanotubes (MWCNT) were used to produce aqueous suspensions. The nanotubes were procured from Helix Material

Solutions Inc., USA. The nanotubes had a specified average outside diameter of 10–20 nm, length of 0.5–40 μm and purity of 95%, produced by chemical vapor deposition (CVD) process. GA fine powder was supplied by Biochemika. Four 500 g samples were prepared with mass fraction of GA and MWCNT as 0.25% and 1%, respectively, however, with varying ultrasonication times including 20, 40, 60, and 80 min. GA was dissolved in DI water using a magnetic stirrer, followed by the addition of MWCNT to the solution. The resulting composition was ultrasonicated for 5 min at 100% amplitude using a 130 W, 20 kHz ultrasonication probe (Sonics & Materials, Inc., USA). As the probe sonicates within a limited conic volume, to facilitate uniform dispersion, sonication was followed by 5 min of magnetic stirring. The ultrasonication and magnetic stirring process were alternated every 5 min until the sample had been sonicated for the desired amount of time. Based on processing time, a certain amount of energy was transferred to each sample. This energy was divided by the mass of the sample (i.e., 500 g) to obtain the specific energy, '*e*' transferred to each sample. It was assumed that all the energy imparted was received by each fluid sample.

Therefore, the samples are defined as:

(a) Sample A: 1 wt% MWCNT, 0.25 wt% GA, ultrasonicated for 20 min, e = 57 J/g.
(b) Sample B: 1 wt% MWCNT, 0.25 wt% GA, ultrasonicated for 40 min, e = 113 J/g.
(c) Sample C: 1 wt% MWCNT, 0.25 wt% GA, ultrasonicated for 60 min, e = 188 J/g.
(d) Sample D: 1 wt% MWCNT, 0.25 wt% GA, ultrasonicated for 80 min, e = 290 J/g.

The samples prepared by this technique were found to be stable for over 1 month with no visible sedimentation or settling.

3.2. Wet-TEM imaging

One of the limitations of the conventional transmission electron microscopy (TEM) technique is that test samples have to be dried and exposed to vacuum before they can be imaged. This may induce structural changes in the sample as compared to the original test fluid. Therefore, one can never be sure whether the dried test sample is representative of the original sample. To overcome this problem, a new type of TEM technique is now available known as wet-TEM. Wet-TEM allows imaging of samples under wet or *in-situ* conditions without altering the original condition of the test fluid. The new technique facilitates the imaging of the actual quality of carbon nanotube dispersion within the base fluid. A wet-cell TEM technique developed by Dongxiang Liao and Jianguo Wen from the Frederick Seitz Materials Research Laboratory at the University of Illinois at Urbana-Champaign was used [24]. A JEOL 2010 LaB6 TEM was used with a beam acceleration voltage of 200 keV. The wet-cell was constructed by holding the fluid between two silicon nitride membrane window TEM grids. The grids contained a 200 μm thick frame and a 50 nm thick window, in which the sample was placed. Thus, even a tiny drop of the sample could be used. The grids were then placed in a custom-built TEM sample holder that included a number of o-rings intended to create a seal against the vacuum for the fluid in the grid.

3.3. Viscosity measurement

The viscosity was measured using a low viscosity rotational type viscometer (LVDV-I Prime, Brookfield Engineering Laboratories, Inc., USA). The model had a maximum torque rating of 0.06737 mN m and a specified accuracy of ±1%, which was verified using a Brookfield's standard viscosity test fluid. A combination of cylindrical sample container and spindle called as UL Adapter was used for taking measurements at low viscosity. The viscous drag experienced by the spindle in UL Adapter was factory calibrated to display dynamic viscosity on a digital output screen. Measurements were taken at several shear rates at 15 and 30 °C.

3.4. Thermal conductivity measurement

The thermal conductivity was measured using a KD 2 Pro thermal properties analyzer (Decagon devices, Inc., USA). The instrument had a probe of 60 mm length and a 1.3 mm diameter and included a heating element, a thermo-resistor and a microprocessor to control and measure the conduction in the probe. The instrument had a specified accuracy of 5%. The samples were maintained at several temperatures using a temperature-controlled chiller. A number of measurements were taken for each sample and a mean of only those measurements with 'R^2' value (correlation coefficient) greater than 0.9995 were considered. The instrument was based on the working principle of a transient hot wire method used in past nanofluid works [1,3,4,25].

3.5. Convective heat transfer measurement

The experimental set up used to measure convective heat transfer coefficient is shown schematically in Fig. 1. The set-up was calibrated to give measurements within 5% accuracy. It consisted of a copper heat transfer section, data acquisition system, a DC power supply, a syringe metering pump and a computer. A straight cop-

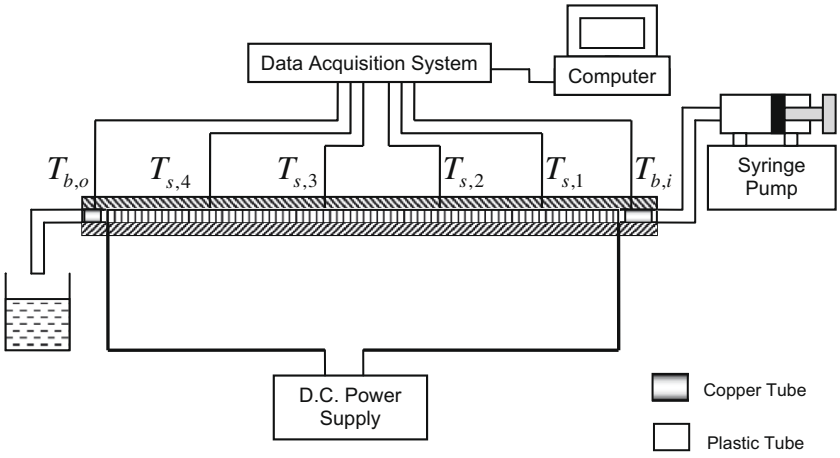

Fig. 1. Schematic for convective heat transfer measurement experimental set-up.

per tube of 914.4 mm length, 1.55 mm inner diameter and 3.175 mm outer diameter was used as a test section. The whole section was heated by an AWG 30 nichrome 80 wire (MWS wire industries, USA) wound on the tube and connected to a 1500 W, 0–300 V, 0–5 A DC power supply (Lambda, USA). Both ends of the copper tube were connected to well-insulated plastic tubing to insulate the heat transfer section and fluid from axial heat conduction, and to avoid heat losses. The experiments were run under constant heat flux conditions using a current of 0.2 A. The test section was insulated to prevent loss of heat to the surroundings. Four surface-mount thermocouples were mounted on the test section at axial positions of 19 cm ($T_{s,1}$), 39.5 cm ($T_{s,2}$), 59 cm ($T_{s,3}$) and 79 cm ($T_{s,4}$) from the inlet of the section to measure wall temperatures. Additionally, two thermocouples were mounted on individual, unheated, and thermally insulated, short copper tubes located before and after the heat transfer section to measure the fluid bulk temperature at the inlet and outlet of the heat transfer section. The fluid was collected in a thermally insulated cup after passing through the heat transfer section where temperature was measured under mixing cup conditions to validate the outlet bulk fluid temperature measured by the thermocouple. The pump used was a Cole Palmer syringe metering pump. The flow rates used were 40, 60 and 80 mL/min such that the flow conditions were always laminar. The corresponding Reynolds number for water at these flow rates are approximately 600, 900 and 1200, respectively. All the thermocouples and the output from the DC power supply were connected to a data acquisition system (Agilent 34970A), which was connected to a computer. The set-up was calibrated both under isothermal and constant heat flux operating conditions, and correction factors were applied to all the measurements.

The convective heat transfer coefficient ($h(x)$) at an axial distance 'x' from inlet is defined as:

$$h(x) = \frac{q''_s}{T_s(x) - T_b(x)} \tag{1}$$

where q''_s, $T_s(x)$ and $T_b(x)$ are heat flux applied to the fluid, wall temperature at a distance 'x' from the inlet, and fluid bulk temperature at a distance 'x' from the inlet, respectively. From the energy balance equation, the bulk temperature of the fluid ($T_b(x)$) at an axial distance, x can be found using:

$$T_b(x) = T_{b,i} + \frac{q''_s.P}{\dot{m}.c_p}x \tag{2}$$

where $T_{b,i}$, P, x, $\dot{m}$ and c_p are fluid bulk temperature at the inlet, perimeter of the copper tube, axial distance from the inlet of the test section, mass flow rate of the fluid, and specific heat of the fluid, respectively. The heat flux applied to the fluid (q''_s) can be found using:

$$q''_s = \frac{\dot{m}.c_p(T_{b,o} - T_{b,i})}{A} \tag{3}$$

The convective heat transfer coefficient is also defined in the form of Nusselt number (Nu) as:

$$Nu(x) = \frac{h(x) \cdot D_i}{k} \tag{4}$$

where D_i and k are the inside diameter of the copper tube and the thermal conductivity of the test fluid, respectively.

4. Results and discussion

4.1. Imaging data

Fig. 2a–d shows the pictures of samples A–D at a scale of 0.5 μm, under *in-situ* conditions, using wet-TEM technique [24]. It can be seen that samples A and B exhibit a good three-dimensional network of carbon nanotubes. Samples C and D show shorter carbon nanotubes which can be attributed to the additional ultrasonication time. From Fig. 2e and f (scale of 200 nm), it appears that the length of the nanotubes is relatively less in sample D than in sample B. The images provide only snapshots of CNT nanofluid samples for different ultrasonication times. Though the images are not entirely representative of all nanofluid samples, they give good indication of the damage caused by excessive ultrasonication. The imaging data also provides some evidence that flow (viscosity) and thermal (i.e., thermal conductivity) properties should be affected by ultrasonication time as shown in the subsequent sections.

4.2. Viscosity data

A rotating drum viscometer was used to measure dynamic viscosity and shear rate. Fig. 3a and b shows the variation of viscosity with shear rate for each of the samples including water and 0.25 wt% GA aqueous solution at 15 and 30 °C, respectively. It can be clearly seen from the figure that that MWCNT aqueous nanofluids displayed a non-Newtonian behavior especially at 15 °C even when taking variability into account as shown by the error bars in Fig. 3a and b. A shear thinning or pseudoplastic behavior was observed resulting in a decrease in viscosity with an increase in shear rate up to 60 s^{-1}. In case of 0.25 wt% GA aqueous solution, shear thinning was observed initially (up to 60 s^{-1}) but a slight shear thickening can be observed at 75 s^{-1}. A shear thinning effect can be explained by possible de-agglomeration of bundled nanotubes or realignment in the direction of the shearing force, resulting in less viscous drag. A slight shear thickening can be attributed to the unique fluid properties Gum Arabic dispersions which have shown both shear thinning and shear thickening behavior at different shear rates in recent studies [26]. More work is required in this area to fully understand the role of Gum Arabic on nanofluids.

Additionally, it is clear that the viscosity of the nanotube suspension first increased from sample A to sample B, and thereafter decreased with increase in ultrasonication time. According to Starr et al. [27], a clustered nanoparticle suspension shows lower viscosity than a dispersed suspension. The increase in viscosity in a dispersed sample is due to increased attractive surface interactions as a result of greater surface-to-volume ratio [27]. For a fully dispersed sample, the total exposed nanoparticle surface is much more than in a clustered sample, resulting in greater viscosity in dispersed samples. Furthermore, in this work it is suggested that due to less dispersing energy used in the preparation of sample A, the nanotubes may not have received enough energy to overcome agglomerization and still remained in a clustered state. On the other hand, sample B was sonicated for more time, and received optimum energy to create a uniform dispersion which resulted in greater viscosity than sample A. After 40 min of sonication, it was seen that the viscosity continuously decreased with further sonication. Another effect is the increased breakage of nanotubes with increase in ultrasonication time as observed in Fig. 2. Excessive ultrasonication results in reduced nanotubes length and aspect ratio. It has also been found by Yang et al. [19] that with increase in ultrasonication of carbon nanotube-in-oil dispersions, viscosity decreases too. They explained this observation based on the disruption of three-dimensional network of nanotubes with a decrease in aspect ratios of nanotubes. This reasoning can also be confirmed by examining all the wet-TEM pictures in Fig. 2.

From the data, a non-Newtonian behavior is observed; however, quantitative assessment requires a correlation between shear stress and shear rate by curve fitting. Plots of shear stress vs. shear rates were made for each sample including 0.25 wt% Gum Arabic.

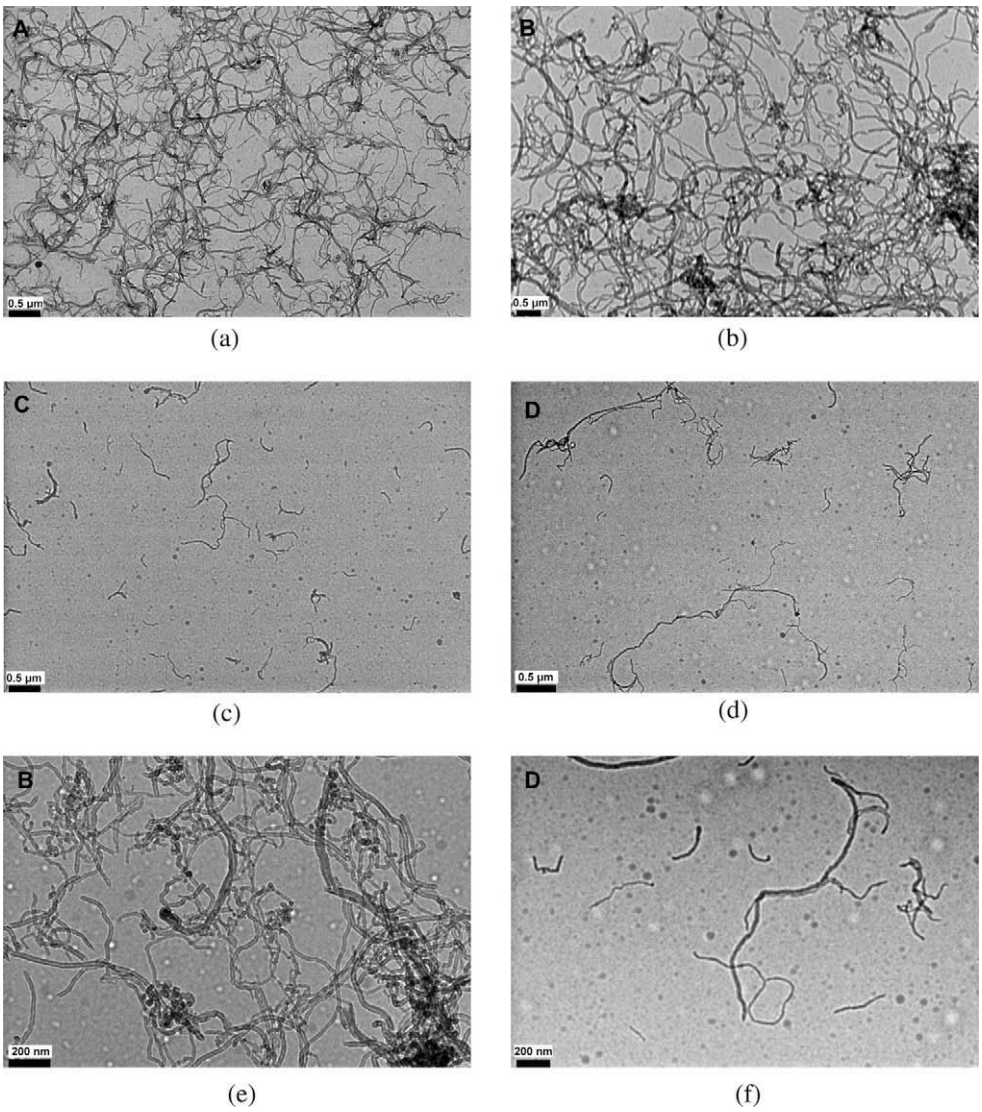

Fig. 2. Wet-TEM images of aqueous suspensions of 1 wt% MWCNT, 0.25 wt% GA sonicated for: (a) 20 min at 0.5 μm scale, (b) 40 min at 0.5 μm scale, (c) 60 min at 0.5 μm scale, (d) 80 min at 0.5 μm scale, (e) 40 min at 200 nm scale, and (f) 80 min at 200 nm scale.

The mathematical relation found for each sample was compared with the viscosity models discussed in Section 2.2, to find out the characteristic flow behavior of the samples. It was found that all the nanofluid samples followed the Power Law ($\tau = K.\dot{\gamma}^n$) viscosity model. The R^2 value (correlation coefficient) for each of the curves was found to be more than 0.999, thus indicating a good correlation even when a slight shear thickening behavior was also observed at 75 s^{-1}. The unit of K is same as that of viscosity and therefore, it is indicative of the magnitude of viscosity for a non-Newtonian fluid. The values for flow consistency index, K and flow behavior index, n were found for each nanofluid sample and 0.25 wt% GA at 15 and 30 °C, as shown in Fig. 4. From the figure, it is seen that flow consistency index increases with the ultrasonication time from sample A–B and thereafter, it decreases. This is in agreement with the viscosity trend observed in Fig. 3a and b. Additionally, the corresponding values for 0.25 wt% GA aqueous solution were found to be lower than the MWCNT nanofluid samples, thus indicating that it is less viscous. From the Fig 4b, the flow behavior index (n) at 30 °C remains almost constant with ultrasonication time. Since a low value of n indicates a more pronounced non-Newtonian behavior, from Fig 4b it can be said that there is a greater degree of non-Newtonian behavior at lower temperatures. However, at both temperatures it is observed that 0.25 wt% GA aqueous solution has a higher value of n than all nanofluid samples, thus indicating a lesser degree of non-Newtonian behavior. Therefore, the non-Newtonian behavior in MWCNT nanofluid samples is not just due to the presence of GA but due also by the inclusion of nanotubes.

4.3. Thermal conductivity data

Measurements were taken for all the nanofluid samples including DI water at different temperature. All measurements for DI water were found to be within 2% of the NIST values. The presence of 0.25% Gum Arabic in water resulted in an insignificant change in the thermal conductivity of water; therefore, water was used as base fluid for comparison purposes. From Fig. 5, the thermal conductivity of the nanofluid samples first increases slightly with temperature, and after 24 °C it increases non-linearly with temperature. One of the suggested reasons behind this phenomenon is the increased Brownian motion effect. Jang and Choi [22] suggested that as the temperature is increased, the viscosity of the nanofluid decreases, which results in an increase in Brownian motion of nanoparticles, which sets convection-like effects result-

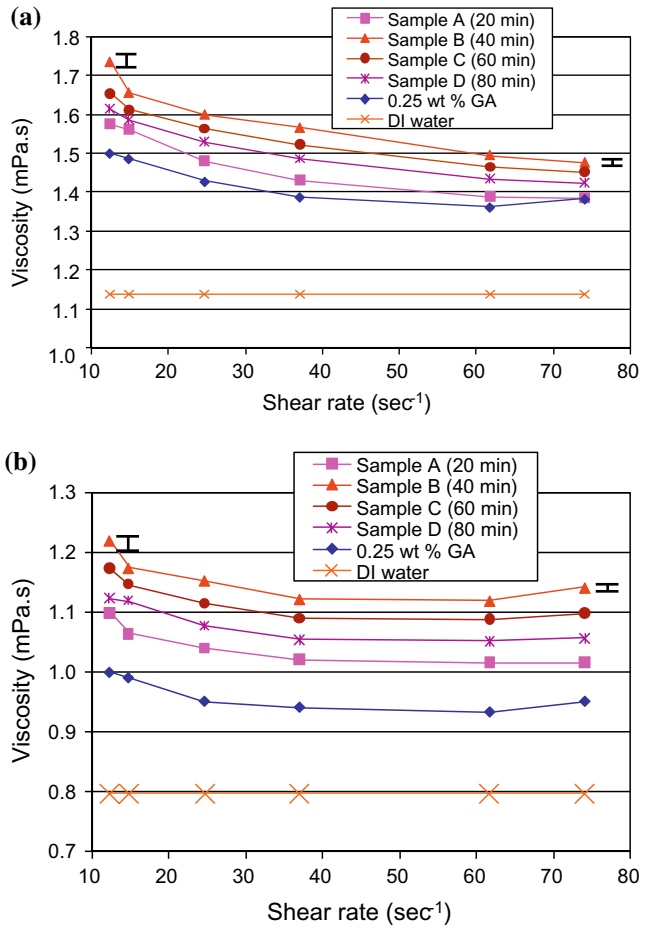

Fig. 3. Variation of viscosity with shear rate at: (a) 15 °C and (b) 30 °C.

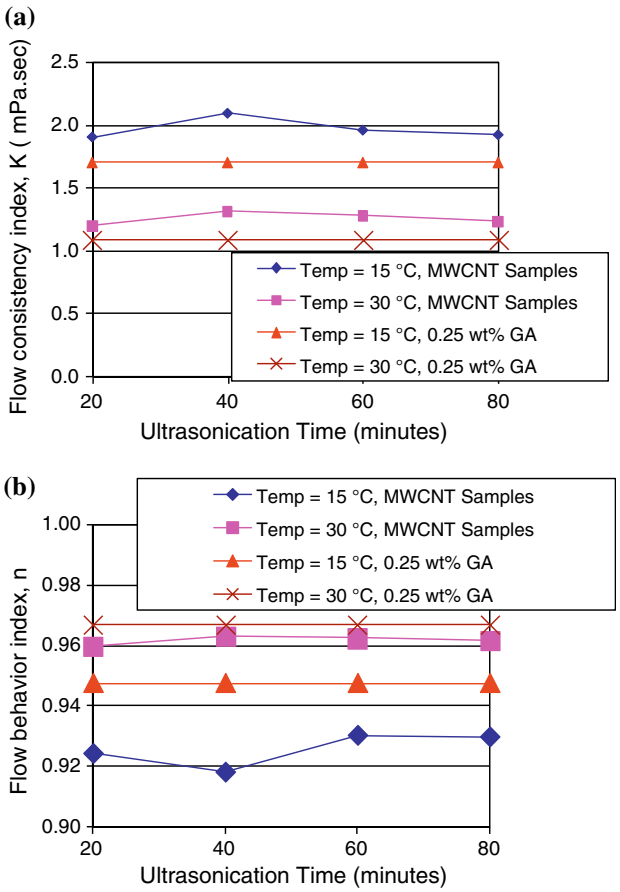

Fig. 4. Variation of: (a) flow consistency index with ultrasonication time and (b) flow behavior index with ultrasonication time.

ing in enhanced thermal conductivity. From the Fig. 5, a maximum increase of 20% in thermal conductivity was obtained for sample B at 35 °C. The average density of MWCNT as provided by the vendor was 2.1 g/cm^3. Taking this value into account, a 1 wt% CNT suspension would be approximately 0.47 by volume (vol %). The percentage enhancement reported by Xie et al. [18] was 7% at 1 vol % of MWCNT (aspect ratio ~ 2000) and that by Assael et al. [1] was 38% at 0.6 vol % MWCNT (aspect ratio ~500). Therefore, it can be said that both Xie el al. [18] and Assael et al. [1] used higher mass fractions of CNTs than in this work. The enhancement values obtained in this work are much better than the value obtained by Xie et al. [18], and slightly less than the value obtained by Assael et al. [1]. However, Assael et al. [1] used a slightly higher volume fraction of MWCNT in his work which could have resulted in a better overall thermal conductivity value. However, the value reported by Ding et al. (i.e., 79% at 1 wt% MWCNT at 30 °C) [4] is much higher than the values obtained in this work even when the concentration of CNTs used in both works is the same. The exact reason for this discrepancy is unclear. It could be suggested that the reason is related to the thermal and physical properties of the CNTs used in both works. Additionally, Ding et al. [4] did not specify the CNT aspect ratio, and it could be different from the aspect ratio (~50–2000) used in this work. From Fig. 5, it can be inferred that thermal conductivity enhancement is affected by ultrasonication time, reaching an optimum for sample B. It is suggested that the reason for this phenomenon is associated with the aspect ratio of CNTs and the quality of three-dimension network established within each of the samples. It was found from wet-TEM imaging that the aspect ratio of CNTs appears to have decreased with ultrasonication. This is evident in Fig. 2 where samples B and D were compared at the 200 nm scale. Assael et al. [1] concluded that a decrease in aspect ratio decreases thermal conductivity enhancement. Additionally, Wen and Ding [2] suggested carbon nanotube networking as one of the factors contributing towards enhanced thermal conductivity as it provides avenues for ballistic or fast heat transport. Sample A shows slightly lower thermal conductivity enhancement because there was not sufficient ultrasonication time or energy to uniformly disperse nanotubes. On the other hand, sample B received sufficient energy for the creation of a uniform and effective three-dimensional network of CNTs. Hence, it can be suggested that there was an optimum condition being established in sample B, where an optimal aspect ratio and a uniform

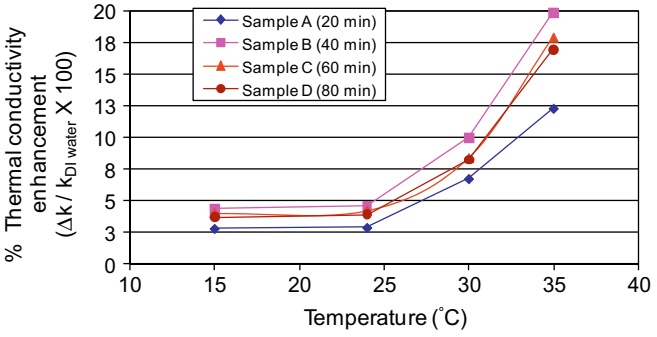

Fig. 5. Variation of percentage enhancement in thermal conductivity with temperature.

three-dimensional network were reached. On further ultrasonic processing, this condition was disturbed which resulted in decreased aspect ratio and a lower quality of three-dimensional network, resulting in a decrease in thermal conductivity enhancement.

4.4. Convective heat transfer data

For the heat transfer experiments, the heat flux was maintained constant at 0.6 W/cm^2. The Reynolds numbers for DI water were found to be approximately 600, 900 and 1200, respectively. The presence of 0.25% Gum Arabic in water resulted in an insignificant change in the heat transfer coefficient of water in laminar flow conditions; therefore, water was used as base fluid for comparison purposes. However, in case of CNT nanofluid as the viscosity of the samples changed appreciably with temperature and shear rate (due to non-Newtonian behavior), the Reynolds number for these samples was found to vary within a range of ±100. Figs. 6 and 7a show the variation of convective heat transfer coefficient of all samples and DI water with respect to non-dimensionalized axial distance, x/D_i for different Reynolds number. Figs. 6 and 7a also indicate the thermal entry length region and thermally fully developed region. It can be seen that the laminar heat transfer coefficient decreases with axial distance. This is expected due to the entry length phenomenon. For a pure Newtonian fluid flowing through a tube with a circular cross section, the flow is considered to be hydrodynamically and thermally fully developed at $x/D_i \geqslant 0.05.\mathrm{Re}$ and $x/D_i \geqslant 0.05.\mathrm{Re.Pr}$, respectively. Once the flow has become fully developed, the heat transfer coefficient value stabilizes for pure fluids. A similar trend is observed for CNT nanofluid samples to a certain extent. A clear enhancement in heat transfer coefficient was observed in the case of CNT nanofluid samples as compared to DI water.

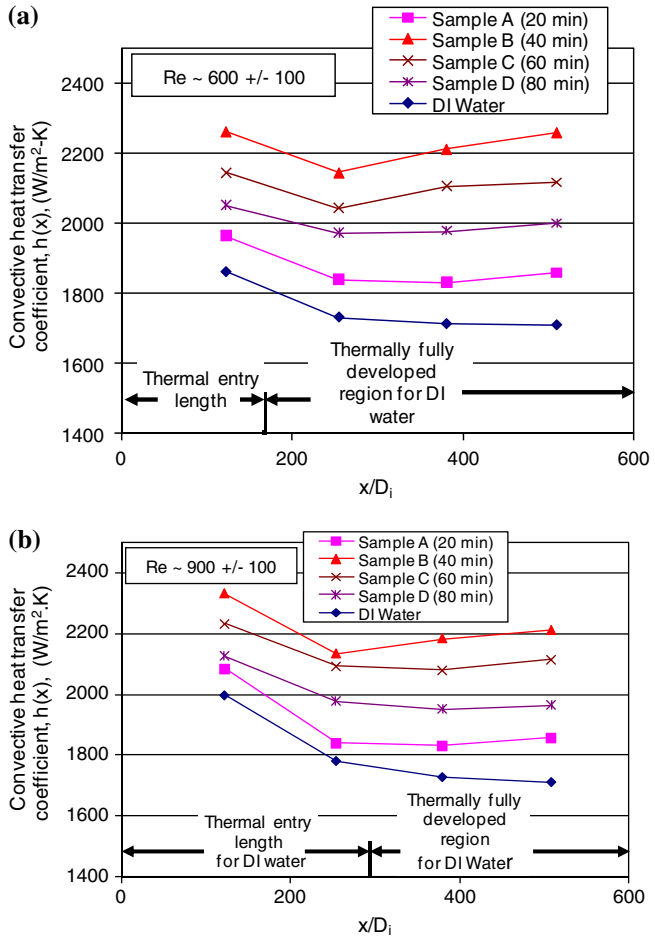

Fig. 6. Axial variation of heat transfer coefficient at: (a) Re ~ 600 ± 100 and (b) Re ~ 900 ± 100.

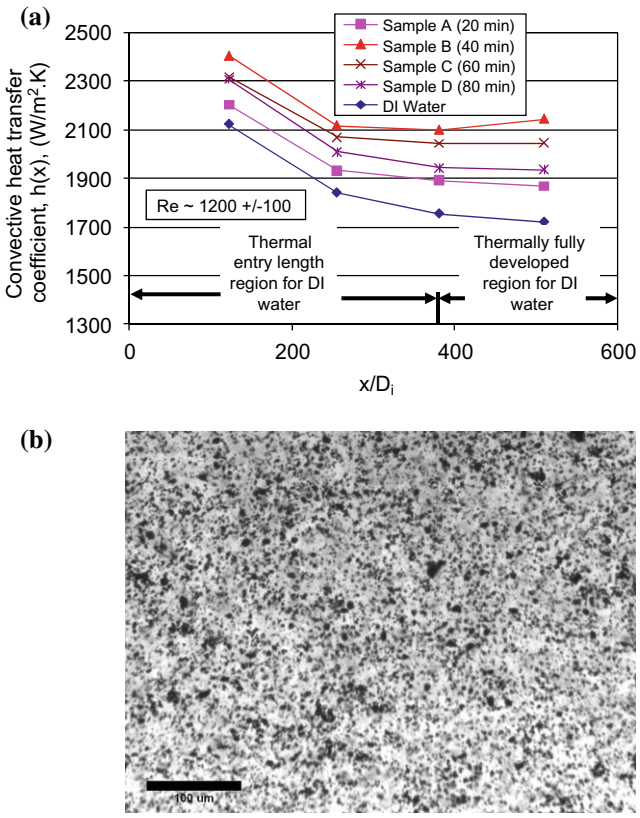

Fig. 7. (a) Axial variation of heat transfer coefficient at Re ~ 1200 ± 100 and (b) microscopic picture of sample B (1 wt% MWCNT, 0.25 wt% GA, 40 min sonication) at 100 μm.

The enhancement in convective heat transfer coefficient increases continuously with axial distance with the maximum increase found to be 32% for sample B at Re ~ 600 ± 100. This increase is more than the maximum increase of 20% in thermal conductivity observed in sample B. These observations were found to both agree and disagree with the previous work for nanofluids. Ding et al. [4] reported similar trends where a more dramatic increase in heat transfer coefficient enhancement (i.e., 375% at 0.5 wt% CNT) as compared to thermal conductivity enhancement (i.e., 37% at 0.5 wt% CNT) were observed. Similar trends were reported by Wen and Ding [16], and Xuan and Li [17]. Wen and Ding [16] reported a heat transfer coefficient enhancement of 47%, and thermal conductivity enhancement of 10% at 1.6 vol % Al_2O_3 spherical nanoparticles in DI water. Xuan and Li [17] reported a heat transfer coefficient enhancement of 60%, and thermal conductivity enhancement of 12.5% at 2 vol % using Cu spherical nanoparticles. In this work, in a similar way, the heat transfer coefficient enhancement has been found to be more than the thermal conductivity enhancement. Ding et al. [4] suggested several possible mechanisms for this observation. Using convective heat transfer fundamentals, Ding et al. [4] stated that the heat transfer coefficient, h can be approximately represented as k/δ_t where k and δ_t are the thermal conductivity of the test fluid and thickness of the thermal boundary layer, respectively. With increase in k and decrease in δ_t or δ, the value of h should increase. A simultaneous de-

crease in δ or δ_t could be suggested as one reason for the observed heat transfer enhancement. This could be explained by a possible boundary layer thinning effect most likely caused by CNTs in the fluid. However, in the fully developed laminar flow region δ_t and δ are not expected to change appreciably, suggesting that other enhancement mechanisms could be at play.

It has been found previously by Sohn and Chen [28] that for a liquid comprising of solid micro-scale particles, thermal conductivity enhancements under shear conditions are greater than those observed under static conditions. This phenomenon was attributed to micro-convective effects due to the presence of an eddy-type convection mechanism. Significant enhancements were seen in their work for samples having Peclet number greater than 300, where Peclet number, Pe is defined as $\frac{\dot{\bar{\gamma}}_f \cdot d_p^2}{\alpha_f}$; where $\dot{\bar{\gamma}}_f$, d_p and α_f are local mean shear rate experienced by fluid, particle diameter and thermal diffusivity of the fluid, respectively. Additionally, Ahuja [29] found that significant enhancements were seen in thermal conductivity in tube flow when the Ahuja number defined as $\phi \cdot \frac{\omega a^2}{\nu_f} \cdot \frac{\omega a^2}{\alpha_f} \cdot \left(\frac{R}{a}\right)^2 \cdot \left(\frac{L}{2a}\right) \times 10^{-8} \times$ *Doublet Collision Frequency ratio* where ϕ, ω, a, ν_f, R and L are particle volume fraction, angular velocity of particles, particle radius, kinematic viscosity, tube radius and heated length, respectively, has a value near to 0.02. The difference between both of these studies was that Sohn and Chen [28] study was based on couette flow whereas Ahuja [29] was based on poiseuille flow. However, both studies explained the enhancement due to the inertia of entrained fluid rotating with the particles. Based on a microscopic picture of a drop of sample B (See Fig. 7b), it was found that the nanotubes in the present study microscopically exist as clusters with a typical size between 10 and 20 μm. This value is much less than the particle sizes of 2.9 and 0.3 mm used by Sohn and Chen [28], and 50 and 100 μm used by Ahuja [29]. Additionally, the particle volume fractions of suspensions used by them were greater than those used in the current study ($\phi = 0.0047$). The Peclet number as defined by Sohn and Chen [28] and the Ahuja number [29] were calculated based on the typical cluster size (10–20 μm), particle volume fraction, and flow conditions. It was found that the Peclet number (0.5–2.5) and Ahuja number (10^{-6}–10^{-7}) were well below the values where significant enhancement could be expected and explained by microconvection. Therefore, a micro-convective effect could not be proposed as one of the major reasons for heat transfer enhancements in our study.

Also, CNTs in the nanofluid could experience a re-arrangement effect due to non-uniform shear rate in the radial direction. As seen in Figs. 3 and 5, the viscosity and thermal conductivity of CNT nanofluids decreases with shear rate, and increases with temperature, respectively. These lead to a non-uniform viscosity and thermal conductivity enhancement in the radial direction. Wen and Ding [30] showed previously that such a change could result in a high Nusselt number and hence, a higher heat transfer coefficient. Thermal convection is improved if the viscosity near the wall of a flowing fluid in a tube is decreased with respect to the viscosity of the bulk fluid [31]. In case of tube flow, the temperatures at the wall and the centerline are maximum and minimum, respectively. Due to these temperature variations, there are variations in viscosity in the radial direction, resulting in minimum viscosity at the wall and maximum viscosity at the centerline. This leads to convective effects in the radial direction, and hence, improved heat transfer coefficient [31]. Additionally, it has been found from past work [32] that a non-Newtonian fluids have a higher Nusselt number than Newtonian fluids. Gingrich et al. [32] found that a fluid with a fluid behavior index, n less than one (indicating shear thinning behavior) exhibits higher heat transfer than one with n equal to unity. Since, CNT-based nanofluids exhibit a shear thinning behavior, it could be said that the non-Newtonian behavior could

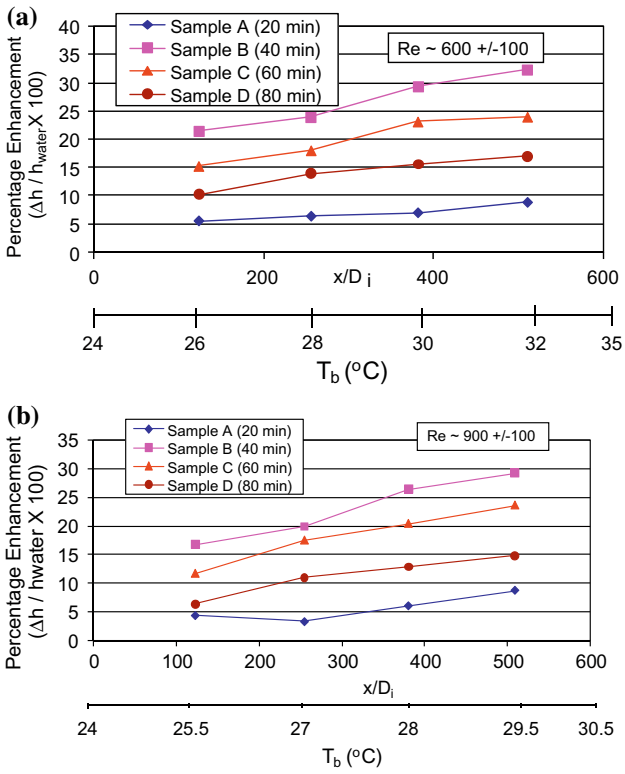

Fig. 8. Axial variation of percentage enhancement in heat transfer coefficient and fluid bulk temperature at: (a) Re ~ 600 ± 100 and (b) Re ~ 900 ± 100.

be a major mechanism behind the higher heat transfer enhancement as compared to thermal conductivity enhancement.

Ding et al. [4] observed that the enhancement of heat transfer coefficient reached a maximum for a certain value of x/D_i. However, in this work, we have found that the percentage enhancement increases continuously with the axial distance as seen in Figs. 8 and 9a. In Figs. 8 and 9a, the bulk temperature of the CNT nanofluid increases with axial distance, which results in a significant increase in the thermal conductivity of the CNT nanofluid as thermal conductivity increases with temperature (Fig. 5). As the heat transfer coefficient of a fluid is directly proportional to thermal conductivity in laminar flow (Eq. (4)), this in turn results in a slight increase in heat transfer coefficient. In addition to measuring the heat transfer coefficient, the local Nusselt number was calculated for each sample to determine the net heat transfer enhancement in a non-dimensionalized way using Eq. (4). The corresponding thermal conductivity values for MWCNT nanofluid samples were calculated by linear interpolation from Fig. 5 after considering the bulk temperature from Figs. 8 and 9a. The Nusselt number values for Re ~ 600 ± 100 are shown in Fig. 9b. It was found that the experimental Nusselt number in the case of DI water matched well with the theoretical fully-developed Nusselt number value of 4.36 for a constant heat flux case. Further, from the Nusselt number calculations, a clear heat transfer enhancement can be seen in Fig. 9b.

Figs. 10 and 11 show the variations for heat transfer coefficient enhancement with Reynolds number for all the nanofluid samples. It can be seen the percentage heat transfer enhancement slightly decreases with increase in Reynolds number. This is can be explained by a decrease in bulk temperature of the nanofluid at a particular x/D_i value with an increase in Reynolds number (Figs. 8 and 9a). It was previously seen that the thermal conductivity enhancement has a considerable dependence on the bulk temperature of the nanofluid. Therefore, due to a decrease in bulk temperature of the nanofluid, its thermal conductivity enhancement should also

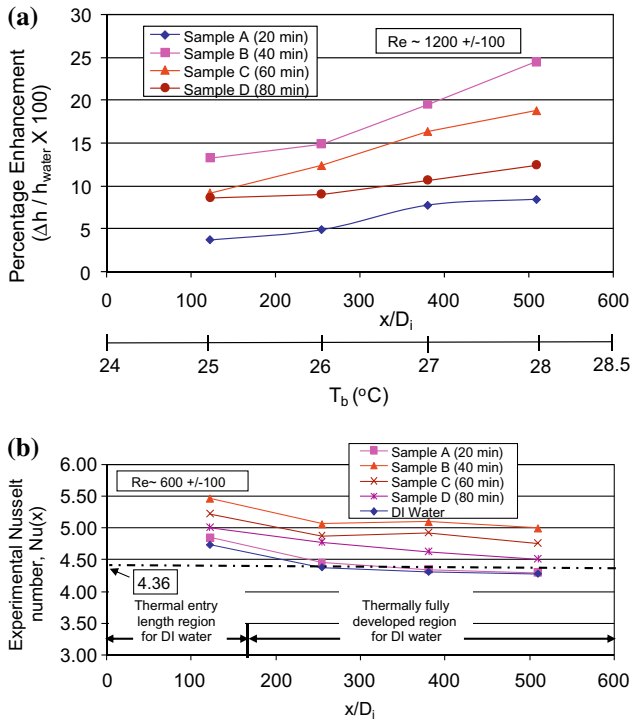

Fig. 9. (a) Axial variation of percentage enhancement in heat transfer coefficient and fluid bulk temperature at Re ~ 1200 ± 100, (b) variation of experimental Nusselt number with axial distance at Re ~ 600 ± 100.

decrease. This results in slight a decrease in heat transfer enhancement. However, as this enhancement reduction was found to be small, further investigation is required.

From Figs. 8 and 9a, it can be inferred that ultrasonication time indirectly affects heat transfer enhancement. The maximum

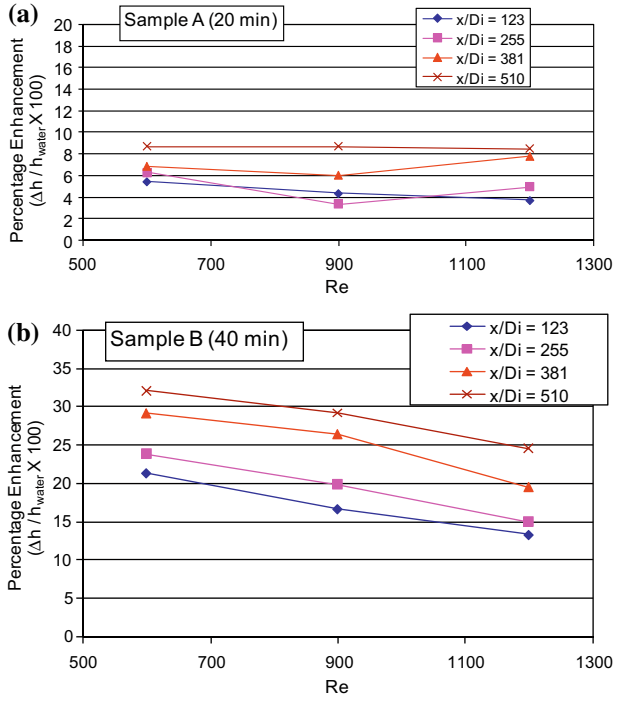

Fig. 10. Variation of percentage enhancement in heat transfer coefficient with Reynolds number: (a) sample A and (b) sample B.

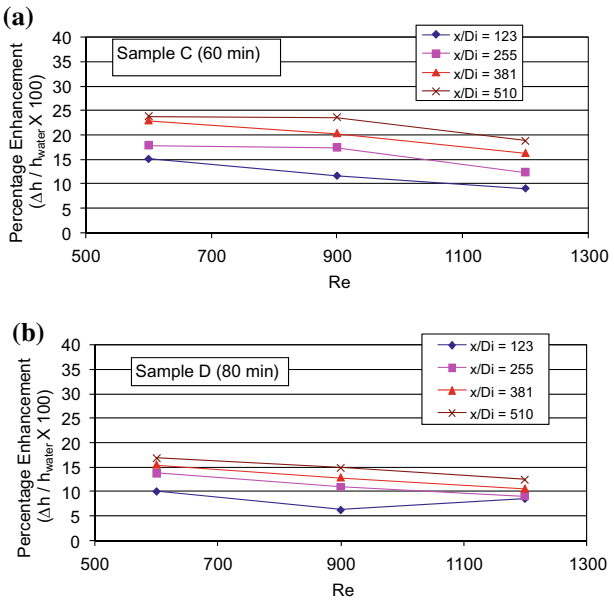

Fig. 11. Variation of percentage enhancement in heat transfer coefficient with Reynolds number: (a) sample C and (b) sample D.

enhancement was observed in sample B. This phenomenon is observed at all the three Reynolds number used in the study. A similar trend was seen in the thermal conductivity data. The reason for the phenomenon could be again associated with the aspect ratio of CNTs and the quality of three-dimension network established within each of the samples, as described in Section 4.3.

5. Conclusions and recommendations for future work

5.1. Conclusions

Through this work, it has been confirmed once again that CNT nanofluids have potential as heat transfer fluids. The aqueous suspensions of multi-walled carbon nanotubes prepared by using Gum Arabic as surfactant were found to be stable for months. However, the preparation method of the nanofluids is an important step affecting the overall heat transfer performance. It was found that at a given CNT composition, there are certain optimum processing conditions (ultrasonication time in this case) which give the maximum enhancement in heat transfer performance. The flowing conclusions are presented:

- Ultrasonication has twofold effect on the CNT nanofluids. Below the optimum processing time, the ultrasonication aids in forming better dispersions, however, once the optimum time has been reached further ultrasonication results in an increased breakage rate of the nanotubes, and hence reduces the aspect ratio of CNTs. In this work, the optimum ultrasonciation time was found to be 40 min at 1 wt% MWCNT concentration, using a 130 W, 20 kHz ultrasonicator.
- Viscosity of the nanofluids increases with sonication time until a maximum value is reached and decreases thereafter. The initial increase is associated with declustering of CNT bundles, resulting in formation of a better dispersion. The later decrease in viscosity can be explained by increased breakage rate of CNTs, resulting in shorter nanotubes, and hence, inferior networking of CNTs in dispersion.
- CNT nanofluids exhibit a shear-thinning (pseudoplastic) non-Newtonian behavior and follow the Power Law viscosity model. The flow consistency index was found to be higher than that of 0.25 wt% Gum Arabic aqueous solution. Also, the flow behavior

index was found to be lower than that of 0.25 wt% Gum Arabic aqueous solution. This shows that the non-Newtonian character in CNT nanofluids could not be solely attributed to the presence of Gum Arabic.
- The maximum percentage enhancement in thermal conductivity was 20%, and was observed in Sample B which was sonicated for 40 min.
- The percentage enhancement in thermal conductivity of CNT nanofluids increases considerably after 24 °C.
- The maximum thermal conductivity enhancement was obtained for an ultrasonication time of 40 min, and was found to decrease with further sonication. The initial increase was explained by formation of better three-dimensional network in the CNT samples, and the later decrease was explained by a decrease in aspect ratio of CNTs.
- The maximum percentage enhancement in heat transfer coefficient was 32% at Re $\sim$ 600 ± 100 and was observed in Sample B.
- The percentage enhancement in heat transfer coefficient at a particular axial distance was found to slightly decrease with an increase in Reynolds number. This effect was attributed to the decrease in thermal conductivity enhancement due to lower bulk temperature of the fluid which decreases with Reynolds number. However, as this decrease was slight, further investigation is still required.
- The percentage enhancement in heat transfer coefficient was found to continuously increase with axial distance. The reason behind the phenomenon is explained by the contribution from a considerable increase in thermal conductivity with an increase in bulk temperature with axial distance.
- The maximum percentage enhancement in heat transfer coefficient (i.e., 32%) was found to be more than the maximum percentage enhancement in thermal conductivity (i.e., 20%). Many possible mechanisms were studied and presented for this phenomenon including the contribution of boundary layer thickness, micro-convective effect, particle rearrangement, possible induced convective effects due to temperature and viscosity variations in radial direction, and non-Newtonian nature of the samples.

5.2. Recommendations for future work

Though from experimental work it is known that nanofluids exhibit enhanced heat transfer performance, the contribution of each proposed physical mechanism still is unknown. Computer simulations that take into account the non-Newtonian characteristic of the nanofluids could give a better understanding of the observed behavior. Other parameters like base fluid type (ethylene glycol, mineral oil, refrigerants), aspect ratio, flow conditions (laminar, transition, turbulent) could provide further understanding of the heat transfer behavior of CNT-based heat transfer fluids.

The experimental data reported previously for nanofluids has large variations. This is due to lack of standardized procedures for preparing nanofluids. An extensive work in this area could help in future research activities as well as supporting commercialization efforts in the area of nanofluids for heat transfer applications.

Acknowledgements

The authors express their deepest thanks to Alex Hays and Ryan Franks of the U.S. Army Corps of Engineers Construction Engineering Research Laboratory; Guillermo Soriano and Landon Sommer from Texas A&M University; Professor B. Jones of the Nuclear, Plasma, and Radiological Engineering Department, and Jianguo Wen, Dongxiang Liao of the Frederick Seitz Materials Research Laboratory at the University of Illinois at Urbana-Champaign for their support. The project was supported by the National Science Foundation, SBIR/STTR program, and the U.S. Army Corps of Engineers.

References

[1] M.J. Assael, C.F. Chen, I. Metaxa, W.A. Wakeham, Thermal conductivity of suspensions of carbon nanotubes in water, Int. J. Thermophys. 25 (4) (2004) 971–985.
[2] D. Wen, Y. Ding, Effective thermal conductivity of aqueous suspensions of carbon nanotubes (carbon nanotube nanofluids), J. Thermophys. Heat Transfer 18 (4) (2004) 481–485.
[3] M.J. Assael, I. Metaxa, J. Arvanitidis, D. Christofilos, C. Lioustas, Thermal conductivity enhancement in aqueous suspensions of carbon multi-walled and double-walled nanotubes in the presence of two different dispersants, Int. J. Thermophys. 26 (3) (2005) 647–664.
[4] Y. Ding, H. Alias, D. Wen, R.A. Williams, Heat transfer of aqueous suspensions of carbon nanotubes (CNT nanofluids), Int. J. Heat Mass Transfer 49 (2006) 240–250.
[5] S.U.S. Choi, Z.G. Zhang, W. Yu, F.E. Lockwood, E.A. Grulke, Anomalous thermal conductivity enhancement in nanotube suspensions, Appl. Phys. Lett. 79 (14) (2001) 2252–2254.
[6] D.J. Faulkner, D.R. Rector, J. Davidson, R. Shekarriz, Enhanced heat transfer through the use of nanofluids in forced convection, in: Proceedings of IMECE, Springer, Berlin, 2004.
[7] J. Hilding, E.A. Grulke, Z.G. Zhang, F. Lockwood, Dispersion of carbon nanotubes in liquids, J. Dispersion Sci. Technol. 24 (1) (2003) 1–41.
[8] R.L. Hamilton, O.K. Crosser, Thermal conductivity of heterogeneous two-component systems, IEC Fundam. 1 (3) (1962) 187–191.
[9] R. Bandyopadhyaya, E. Nativ-Roth, O. Regev, R.Y. Rozen, Stabilization of individual carbon nanotubes in aqueous solutions, Nano Lett. 2 (1) (2002) 25–28.
[10] B.C. Pak, Y.L. Cho, Hydrodynamic and heat transfer study of dispersed fluids with submicron metallic oxide particles, Exp. Heat Transfer 11 (2) (1998) 151–170.
[11] S.K. Das, N. Putra, W. Roetzel, Pool boiling characteristics of nano-fluids, Int. J. Heat Mass Transfer 46 (5) (2003) 851–862.
[12] C. Li, M. Akinc, J. Wiench, M. Pruski, C.H. Schilling, Relationship between water mobility and viscosity of nanometric alumina suspensions, J. Am. Ceram. Soc. 88 (10) (2005) 2762–2768.
[13] S.Z. Heris, S.G. Etemad, M.N. Esfahany, Experimental investigation of oxide nanofluids laminar flow convective heat transfer, Int. Commun. Heat Mass Transfer 33 (4) (2006) 529–535.
[14] D.P. Kulkarni, D.K. Das, G.A. Chukwu, Temperature dependent rheological property of copper oxide nanoparticles suspension (nanofluid), J. Nanosci. Nanotechnol. 6 (4) (2006) 1150–1154.
[15] A. Einstein, Eine neue Bestimmung der Molekuldimension, Annalen der Physik 19 (1906) 289–306.
[16] D.S. Wen, Y.L. Ding, Experimental investigation into convective heat transfer of nanofluids at entrance area under laminar flow region, Int. J. Heat Mass Transfer 47 (24) (2004) 5181–5188.
[17] Y.M. Xuan, Q. Li, Investigation on convective heat transfer and flow features of nanofluids, ASME J. Heat Transfer 125 (2003) 151–155.
[18] H. Xie, H. Lee, W. Youn, M. Choi, Nanofluids containing multiwalled carbon nanotubes and their enhanced thermal conductivities, J. Appl. Phys. 94 (8) (2003) 4967–4971.
[19] Y. Yang, E.A. Grulke, Z.G. Zhang, G. Wu, Thermal and rheological properties of carbon nanotube-in-oil dispersions, J. Appl. Phys. 99 (2006) 1114307-1–1114307-8.
[20] S. Berber, Y.K. Kwon, D. Tomanek, Unusually high thermal conductivity of carbon nanotubes, Phys. Rev. Lett. 84 (20) (2000) 4613–4616.
[21] T. Ohara, D. Suzuki, Intermolecular energy transfer at a solid–liquid interface, Nanoscale Microscale Thermophys. Eng. 4 (3) (2000) 189–196.
[22] S.P. Jang, S.U.S. Choi, Role of brownian motion in the enhanced thermal conductivity of nanofluids, Appl. Phys. Lett. 84 (21) (2004) 4316–4318.
[23] P. Keblinski, S.R. Phillpot, S.U.S. Choi, J.A. Eastman, Mechanisms of heat flow in suspensions of nano-sized particles (nanofluids), Int. J. Heat Mass Transfer 45 (4) (2002) 855–863.
[24] R. Franks, S. Morefield, W. Jianguo, D. Liao, J. Alvarado, M. Strano, C. Marsh, A study of nanomaterial dispersion in solution by wet-cell transmission electron microscopy, J. Nanosci. Nanotechnol. 8 (1–4) (2008).
[25] A. Alloush, W.B. Gosney, W.A. Wakeham, A transient hot wire instrument for thermal conductivity measurements in electrically conductivity instruments in elevated temperatures, Int. J. Thermophys. 3 (3) (1982) 225–235.
[26] C. Sanchez, D. Renard, P. Robert, C. Schmitt, J. Lefebvre, Structure and rheological properties of acacia gum dispersions, Food Hydrocolloids 16 (2002) 257–267.
[27] F.W. Starr, J.F. Douglas, S.C. Glotzer, Origin of particle clustering in a simulated polymer nanocomposite and its impact on rheology, J. Chem. Phys. 119 (3) (2003) 1777–1788.
[28] C.W. Sohn, M.M. Chen, Microconvective thermal conductivity in disperse two phase mixture as observed in a low velocity couette flow experiment, J. Heat Transfer Trans. ASME 103 (1981) 47–51.
[29] A.S. Ahuja, Augmentation of heat transfer in laminar flow of polystyrene suspensions. II. Analysis of the data, J. Appl. Phys. 46 (8) (1975) 3417–3425.

[30] D.S. Wen, Y.L. Ding, Effect on heat transfer of particle migration in suspensions of nanoparticles flowing through minichannels, Microfluidics Nanofluidics 1 (2) (2005) 183–189.
[31] W. Kamil, Heat transfer in temperature-dependent non-newtonian flow, Chem. Eng. Process. 43 (2004) 1223–1230.
[32] W.K. Gingrich, Y.I. Cho, W. Shyy, Effect of shear thinning on laminar heat transfer behavior in a rectangular duct, Int. J. Heat Mass Transfer 35 (11) (1992) 2823–2836.